Double-pass amplification of picosecond pulses with a tapered semiconductor amplifier

Research Article | Vol. 27, No. 21 / 14 October 2019 / Optics Express 30752
Optics EXPRESS

Double-pass amplification of picosecond pulses with a tapered semiconductor amplifier

ADAM F. FORREST,[1,2,*] MICHEL KRAKOWSKI,[3] PAOLO BARDELLA,[4] AND MARIA ANA CATALUNA[1,2]

[1] *Institute of Photonics and Quantum Sciences, School of Engineering and Physical Sciences, Heriot Watt University, Edinburgh Campus, Edinburgh, EH14 4AS, United Kingdom*
[2] *previously also with the School of Engineering, Physics and Mathematics, University of Dundee, Dundee, DD1 4HN, United Kingdom*
[3] *III-V Lab, 1 Avenue Augustin Fresnel, Campus de Polytechnique, 91767 Palaiseau, France*
[4] *Dipartimento di Elettronica e Telecomunicazioni, Politecnico di Torino, I-10129, Turin, Italy*
[*] *adam.forrest@hw.ac.uk*

Abstract: Double-pass amplification of picosecond pulses is demonstrated and compared with single-pass amplification. This was achieved using a two-section tapered semiconductor optical amplifier with a chirped quantum-dot active region and a mode-locked laser diode as a seed. Across the range of biasing conditions common to both configurations, an enhancement in signal gain of up to 7 dB and output power by a factor of 4.1 was seen in the double-pass amplifier, compared to the single-pass. Only marginal increases in pulse duration were observed in the double-pass regime compared to the single-pass amplifier, meaning that enhancements in output power were well translated into peak power. Furthermore, the two-section contact layout of the SOA allowed the pulse duration to be optimised for a given fixed output power, giving additional flexibility to the amplifier. These results demonstrate the suitability of this simple and versatile technique, which could become the new standard in amplification of ultrashort pulses.

1. Introduction

The use of tapered semiconductor optical amplifiers (SOAs) for the amplification of ultrashort pulses offers a number of advantages due to their low-cost, small footprint, efficiency and simplicity. Furthermore, the tapered waveguide geometry, which is designed to support a solitary transverse optical mode, allows for a large active area and hence increased output power, whilst maintaining a reasonable beam quality. Tapered SOAs have been used to boost the power of a wide variety of laser platforms, including semiconductor edge-emitting diodes [1] and disk lasers [2], as well as Ti:Sapphire lasers [3,4]. For example, a semiconductor tapered SOA was used to boost the power of an optical frequency comb while maintaining optical phase coherence [3], with the same system also demonstrating its versatility to enhance the power of a spectral window of supercontinuum light [3]. More recently, a tapered SOA was one of the core components in the demonstration of the highest peak power (9 kW) available from an ultrafast edge-emitting semiconductor laser diode system [1].

Quantum-dot (QD) SOAs, which typically have a broad gain bandwidth and short gain recovery times [5], have shown great promise in the context of ultrashort pulse amplification and are particularly well adapted to amplifying high repetition rate sources such as mode-locked laser diodes (MLLDs). Indeed, there have been many promising reports of ultrashort pulse amplification using QD SOAs [6–10]. These have covered pulse repetition rates ranging from 0.6–1.1 GHz [6] up to 80 GHz [10]. A tapered SOA which implemented a chirped active region has also been used to amplify pulses over a broad wavelength range between 1214–1274 nm

#374152 https://doi.org/10.1364/OE.27.030752
Journal © 2019 Received 30 Jul 2019; revised 9 Sep 2019; accepted 26 Sep 2019; published 9 Oct 2019

Optics EXPRESS

using a tunable MOPA setup, showing their spectral versatility [7]. Last among these highlights was the amplification of picosecond pulses from a tapered QD laser up to a peak power of 42 W using a tapered QD SOA [9].

Implementing tapered SOAs in a double-pass amplifier configuration is one method that could potentially improve gain and output power relative to standard MOPA setups, particularly for low input powers. Such improvements have been demonstrated for CW input signals at 780 nm in [11,12], as well as for longer wavelengths in the infrared [13]. A double-pass configuration has also been used to amplify and shape chirped nanosecond pulses [14], but as yet there have been no reports of using such an amplification regime for ultrashort pulses.

In this paper, a QD two-section tapered SOA is deployed in a double-pass configuration to amplify picosecond pulses generated by a MLLD. A comparison is made with a standard single-pass amplifier set-up, which highlighted relative enhancements in the gain and output power from the double-pass system with minimal disruption to pulse duration.

2. Experimental setup

2.1. Seed laser

The ultrashort pulse source used in this work was a multi-section narrow-ridge MLLD with a multi-layer InAs QD active region. The wafer growth and device processing of this seed laser were performed by Innolume GmbH. For the purposes of this investigation, a combination of bias conditions that produced a stable mode-locked output was selected and kept constant throughout the study. The laser emitted pulses with a repetition rate around 5 GHz, with a central emission wavelength around 1258 nm. The full-width half-maximum optical bandwidth and pulse duration were approximately 4.5 nm and 2.3 ps respectively. These characteristics resulted in a time-bandwidth product of 2.0, indicating that the pulses were fairly chirped (assuming a $sech^2$ pulse shape). The average optical power of the pulses was 2.5 mW (as measured after a single stage optical isolator).

2.2. SOA

A schematic diagram of the tapered SOA used in this investigation is shown in Fig. 1(a). The wafer was grown by Innolume GmbH and was then processed by III-V Lab. At the rear of the device was a 0.5 mm long straight ridge segment with a ridge width of 14 µm. This was followed by the first of two tapered segments, which had a length of 0.5 mm and a full angle of 3°. The final tapered segment had a full flare angle of 0.8° and ran along the remaining 5 mm of the device length, resulting in a front facet width of 110 µm. A shallow ridge was etched into the contact layer at the external limits of the waveguide so as to introduce a slight index guiding effect. This feature, along with the unique waveguide geometry, was implemented based on simulations similar to those performed in [15], with the goal of simultaneously enhancing both gain and beam quality from the tapered facet. An isolation trench was etched into the waveguide 1.875 mm from the rear facet of the device in order to form two electrically isolated contacts which could be independently biased to enhance versatility.

The active region of the tapered SOA contained ten layers of InAs QDs, capped by layers of $In_{0.15}Ga_{0.85}As$ and separated by GaAs barriers. Unlike the active region of the seed laser, the QD layers in the SOA were non-identical and had a chirped structure whereby the average size of the dots in each layer was varied by altering the thickness of the $In_{0.15}Ga_{0.85}As$ capping layer. As a consequence, the central wavelength of the ground state emission from the different QD layers also varied. The ten QD layers that made up the active region of the SOA were subdivided into three groups based on their target ground state emission wavelength. The three QD layers closest to the p-contact of the device were designed to have a ground state emission wavelength of 1211 nm. Directly following these layers were three layers of QDs with a target ground state

Optics EXPRESS

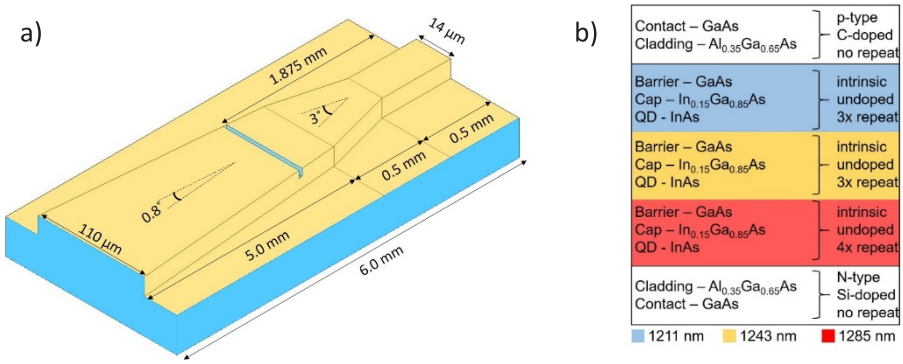

Fig. 1. (a) Schematic diagram of the tapered SOA, fabricated by III-V Lab (not to scale, waveguide tilt not shown). (b) Schematic illustration of the epitaxial structure used to fabricate the tapered SOA (grown by Innolume GmbH).

emission wavelength of 1243 nm. The final four QD layers were tuned to produce ground state emission centred at 1285 nm. This chirped active region design was implemented in order to broaden the gain bandwidth and therefore the versatility of the SOA, allowing for a broader range of signal wavelengths to be amplified.

The waveguide of the SOA was at an angle of 7° with respect to its facets, on top of which anti-reflective coatings were deposited in order to reduce reflectivity as much as possible. This was done to supress solitary lasing and optimise input and output coupling efficiency. The SOA was mounted on a copper heat sink and was maintained at a constant temperature of 20°C by a Peltier cooler and temperature controller throughout this work. Both the front and rear sections of the device were driven by CW constant current diode drivers.

2.3. Amplifier configurations

Schematic diagrams of both the single and double-pass amplifier configurations that were investigated in this work are shown in Fig. 2. The single-pass amplifier configuration followed a conventional MOPA set-up in which signal pulses from the seed laser were input coupled into the narrow rear facet of the SOA, amplified over a single pass and then output coupled from the tapered facet. A single stage optical isolator was used to protect against light emitted from the rear of the SOA inadvertently being coupled into the seed laser and disrupting mode-locked operation. The beam was folded and re-routed via various steering mirrors in order to share the setup with the double-pass configuration, but in practice this could be simplified.

In the double-pass configuration, signal pulses were input coupled through the tapered facet of the SOA and amplified during a first pass through the device. Pulses were then output and recoupled into the rear facet of the SOA via a silvered mirror to be amplified again during a second pass, before being output from the tapered facet. The simultaneous input and output coupling of signal and amplified pulses respectively from the same facet of the SOA was made possible by the one-way optical gate that was implemented in the set-up (inset of Fig. 2). This one-way optical gate was comprised of two half-wave plates, a linear polariser, a Faraday rotator and a polarising beam splitter cube. Linearly polarised light from the seed laser that enters the amplification system (from the right hand side of Fig. 2) has its polarisation angle adjusted by the first half-wave plate so that it is completely transmitted by the polarising beam splitter cube. The Faraday rotator then rotates the polarisation angle anti-clockwise by 45° to match the orientation of the linear polariser, before the second half-wave plate adjusts the polarisation angle, in this case to match the polarisation of the SOA. Light that enters the system from the left hand side, such as the amplified pulses from the SOA, has its polarisation angle adjusted by the half-wave

Optics EXPRESS

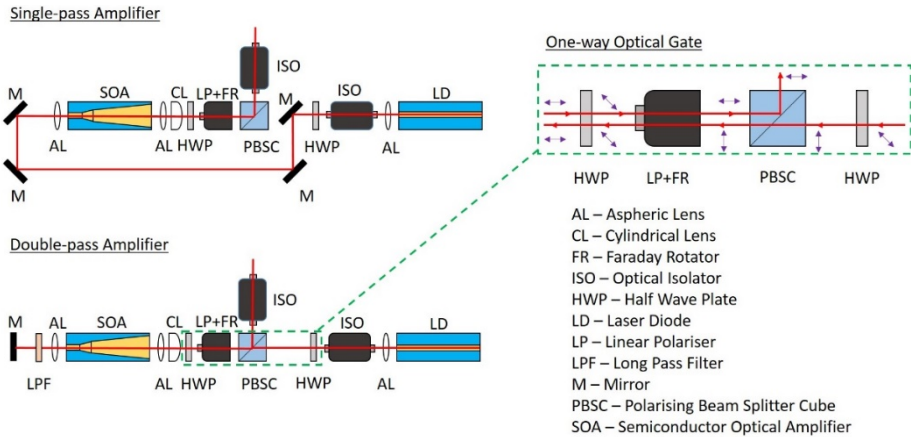

Fig. 2. Amplifier configurations schematic diagrams.

plate to match the orientation of the linear polariser. The Faraday rotator then introduces another 45° anti-clockwise rotation to the polarisation angle so that now, light is completely reflected by the polarising beam splitter cube and exits the system.

A combination of cylindrical and aspheric lenses were used in both configurations to input/output couple light to/from the tapered facet of the SOA. The cylindrical lens was utilised to correct the common beam astigmatism intrinsic to such tapered amplifiers. All measurements of output power in this work were taken after the optical isolator, using a broadband thermal detector (as opposed to a semiconductor based detector, which could introduce inaccuracies arising from inherent spectral sensitivity). In order to determine what fraction of the total measured output

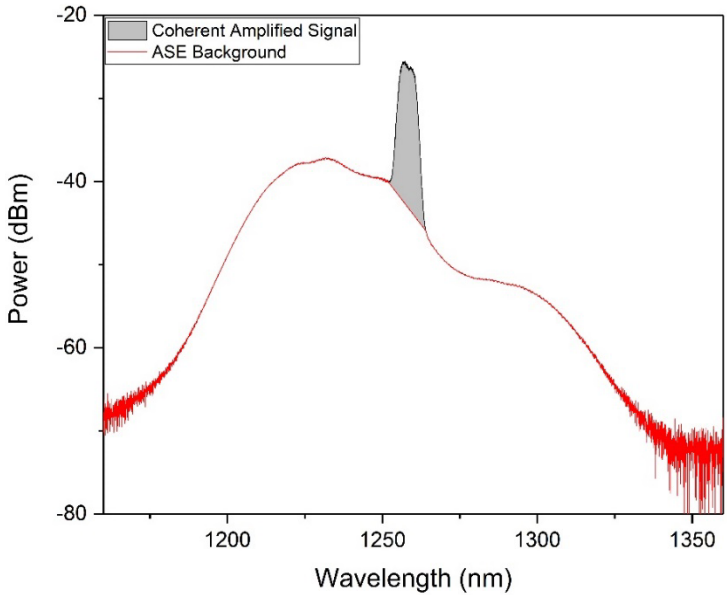

Fig. 3. Typical optical spectrum of an amplified pulse from the single pass configuration. The coherent amplified signal is indicated by the grey shaded area and sits on top of the ASE background shown in red.

Optics EXPRESS

power was coherent amplified signal, as opposed to amplified spontaneous emission (ASE) background, corresponding optical spectra were taken for each output power measurement. An example of such a spectrum is shown in Fig. 3. The spectral method was used in order to separate the ASE and signal components and to calculate the coherent amplified signal power. This method was rigorously demonstrated in [16] and successfully implemented in the context of amplification of picosecond pulse trains in [9,16–19]. In order to implement the method, output spectra (including both ASE and signal) were linearized, normalized and integrated to give the total area under the plot. Then, the coherent amplified signal was removed and the ASE baseline was linearly interpolated before being integrated to give the area under the baseline. Dividing the area under the baseline by the total area gives the fraction of the output power that was ASE background, which was subtracted from 1 and multiplied by the total measured output power to give the coherent amplified signal power (referred to as the output power throughout this paper).

3. Double-pass SOA performance

To begin, the output power from both configurations was measured at various combinations of front and rear section driving currents applied to the SOA. Fig. 4(a) and 4(c) shows plots of output power vs front section driving current at various fixed rear section currents for both amplifier configurations at similar input powers of around 2 mW. Both setups had similar trends of increasing output power with increasing front and rear section driving current, with output powers in the double-pass configuration generally exceeding output powers from the single-pass at equivalent biasing conditions. Across this range of biasing conditions common to both configurations, the relative enhancement in the output power from the double-pass amplifier compared to the single-pass tended to increase with both front and rear section current. The maximum outright improvement in output power was observed at 0.1/4.25 A of rear/front section current, where a relative output power enhancement of 57 mW from 21 mW in the single-pass up to 78 mW in the double-pass amplifier was observed. This corresponded to a proportional improvement by a factor of 3.7, which was slightly short of the maximum proportional enhancement by a factor of 4.1 at 0.1/3.75 A of rear/front section current.

These improvements in output power from the double-pass amplifier compared to the single-pass were also reflected in the signal gain of both configurations. The signal gain was calculated simply by dividing the output power by the input power and so is inclusive of any losses due to coupling light to the SOA and transmission through the various optical components in the systems. Shown alongside the output power plots in Fig. 4 are the corresponding plots of signal gain vs front section current at various fixed rear section currents. For the majority of biasing conditions that were common to both configurations, the double-pass amplifier had a gain that was approximately 3 dB greater than the single-pass. This implies that generally, the double-pass set-up provided around twice the gain of the conventional single-pass amplifier. Furthermore, the maximum gain enhancement offered by the double-pass configuration at a common set of bias conditions was 6.8 dB. The direct comparison with an equivalent single-pass amplifier presented here has served to highlight the attractive benefits offered by a double-pass set-up with regards to boosting output power and signal gain.

As indicated by the plots in Fig. 4(a) and 4(c), the range of driving currents that could be applied to the SOA in the double-pass configuration was limited compared to the single-pass. This was a consequence of the feedback of ASE introduced in the double-pass configuration, which, at higher current levels, resulted in laser emission at wavelengths near the ASE peak of the SOA. Not only did this laser emission reduce the gain at the signal wavelength, it also introduced a significant CW background to the amplified pulses, which manifested in a deterioration of the measured RF spectra and autocorrelation traces. These problems were heightened in this work as a result of the spectral mismatch between the signal wavelength and the peak ASE wavelength of the SOA. We have previously reported a comprehensive study of the amplified

Optics EXPRESS

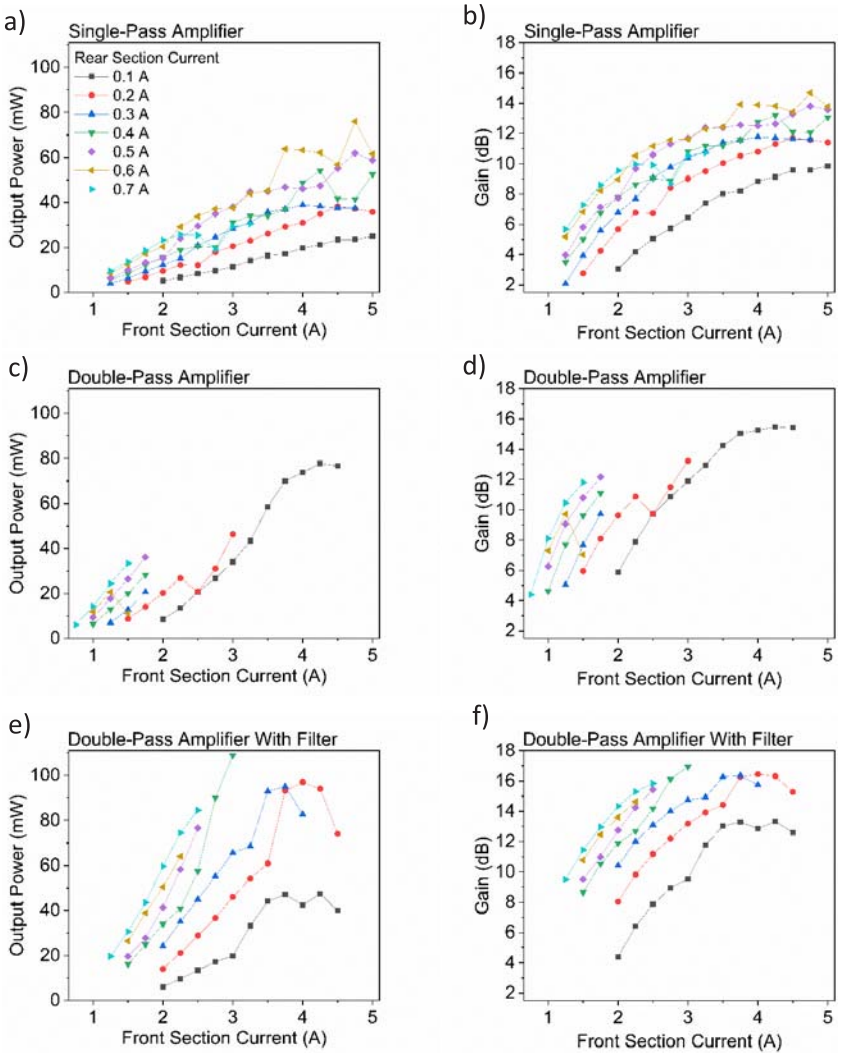

Fig. 4. Plots of average power and gain vs front section current at various fixed rear section currents and a constant input power around 2 mW. (a) Single-pass output power. (b) Single-pass gain. (c) Double-pass output power. (d) Double-pass gain. (e) Double-pass output power with long-pass filterEurope. (f) Double-pass gain with long-pass filter.

spontaneous emission from this device [20]. During that work, extremely broad ASE spectra with spectral bandwidths up to 79 nm were observed, spanning the wavelength range from 1222 nm to 1301 nm, highlighting the potential for the SOA to amplify a variety of sources over a broad range of wavelengths. However, under moderate to high driving currents (above 2 A in the front section and 0.2 A in the rear section) the ASE spectra became dominated by a narrower peak with a spectral bandwidth of around 20-30 nm centred around 1235 nm. This 1235 nm peak is significantly detuned from the 1258 nm seed pulses considered in this work, which contributed to the limited operating range of the double-pass amplifier. In an attempt to increase the driving currents that could be applied to the SOA in the double-pass regime, a long-pass filter with a cut-off wavelength of 1250 nm (FEL1250, Thorlabs) was introduced into the set-up between the

Optics EXPRESS

rear facet of the SOA and feedback mirror. With the filter in place, feedback at the ASE peak at 1235 nm was blocked whilst still allowing the transmission of the signal wavelength at 1258 nm.

Figures 4(e) and 4(f) show plots of the output power and signal gain of the double-pass amplifier with the long-pass filter versus front section current at various fixed rear section currents at an input power around 2 mW. From these plots, it is immediately clear that the inclusion of the long-pass filter greatly increased the operating range of the double-pass amplifier, particularly at rear section currents above 0.1 A. As a result, higher driving currents were delivered to the SOA and the maximum output power was improved. In the single-pass configuration, a maximum output power of 76 mW was observed at a rear/front section current of 0.6/4.75 A. Without the long-pass filter, the double-pass configuration was barely able to better this, reaching a maximum output power of 78 mW at 0.1/4.25 A of rear/front section current. However, with the addition of the long-pass filter, the double-pass configuration was able to reach a maximum output power of 109 mW at 0.4/3.25 A of rear/front section current. This highlights the versatile nature of the double-pass configuration presented here, which was easily customisable with a simple long-pass filter, extending both the operating range and maximum achievable output power of the system.

Across the new extended range of biasing conditions common to both amplifiers, the maximum outright relative enhancement in output power from the double-pass over the single-pass was 75 mW, which was observed at 0.4/3.25 A of rear/front section driving current and marked a proportional increase by a factor of 3.2. This was just short of the maximum proportional increase by a factor of 3.3 which was observed at 0.7/2.5 A of rear/front section current. With regards to the signal gain, a general enhancement of around 4 dB and a maximum enhancement of 7 dB in the double-pass configuration with the filter compared to the single-pass was observed, marking a slight improvement over the double-pass setup without the filter. A potential limitation of the gain enhancements achieved by the double-pass amplifier compared to the single-pass was the fact that, even at the lowest driving currents tested, the double-pass amplifier appeared to operate in a regime of gain saturation. Furthermore, the intrinsic losses associated with input coupling back into the rear facet of the SOA and transmission through the long pass filter also act to limit relative enhancements in signal gain.

These results are summarised in the plots of output power against front section current at rear section currents of 0.1 A and 0.3 A in Fig. 5 where single-pass and double-pass configurations are compared, both with and without the long-pass filter (at similar input power of around 2 mW). As can be seen from these plots, at 0.1 A of rear section current, the operating range of the double-pass configuration was largely unaffected by the presence of the filter. As a result, the relative enhancement of the output power in the double-pass amplifier including the filter was reduced due to losses associated with transmission through the filter. Conversely, at 0.3 A of rear section current, the operating range of the double-pass amplifier was so severely limited without the long-pass filter that significant enhancements in the output power were only achieved with its inclusion in the setup. The plots shown in Fig. 5 also serve to show the lower operation currents in the double-pass configuration required to achieve the same performance as the single-pass. Not only does this yield a wall-plug efficiency advantage derived from the lower electrical power required to drive the SOA, but also from the lower power requirements to stabilize its temperature. Moreover, this results as well in a longer lifetime and minimizes other thermally induced effects caused by a higher active region temperature. All of these factors could be very advantageous in the field deployment of such systems.

Throughout this investigation, the durations of the amplified pulses from both configurations were measured using an autocorrelator. Compared to the input pulse duration of 2.2 ps, both amplifiers produced pulses with increased durations across the entire range of bias conditions. Both configurations also showed a similar trend of increasing pulse duration with increasing front section driving current, albeit with some local fluctuations. This general trend was likely due to the combined effects of gain saturation, self-phase modulation (SPM) and chromatic

Optics EXPRESS

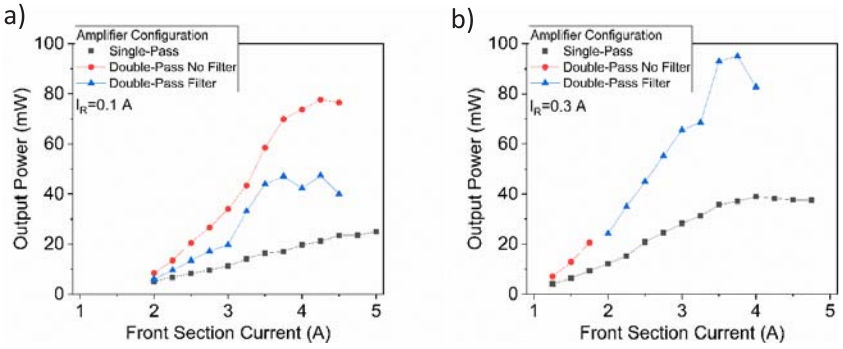

Fig. 5. Comparison of the output power vs front section current plots from the single-pass and double-pass configurations with and without the long-pass filter at rear section currents of 0.1 A (a) and 0.3 A (b).

dispersion, resulting in increased pulse broadening [21]. These effects were more prominent in the double-pass configuration due to the fact that pulses had to propagate through twice the length of gain medium compared to in the single-pass amplifier. This manifested in the observation of marginally longer pulse durations from the double-pass system relative to the single-pass. In the single-pass configuration, across the entire range of bias conditions, the duration of output pulses ranged from 2.3-2.7 ps, whereas pulses from the double-pass set-up had durations ranging from 2.4-3.1 ps. These results were also reflected in the spectral characteristics of the amplified pulses from both configurations, with slightly increased spectral bandwidth pulses being observed from the double-pass set-up. The direct comparison between the single and double-pass configurations serves to illustrate further the advantages of the double-pass set-up of enhanced output power and gain while introducing minimal temporal broadening, therefore preserving enhancements to the peak power.

Figure 6 shows a plot of the duration vs output power of pulses emitted from the double-pass amplifier with the long-pass filter. As can be seen from these plots, the pulse duration tended to increase with increasing output power, which generally corresponded to increased SPM and dispersion with increasing driving current. However the relationship between pulse duration and both front and rear section driving current was relatively complex, something which has been observed in a standard MOPA setup implementing a tapered QD SOA [9]. This complexity was thought to be a reflection of several interlinked factors that affect the level of SPM and gain saturation, and therefore the pulse duration, that amplified pulses encounter during propagation through the double-pass configuration. Firstly, the tapered geometry of the SOA results in non-uniform levels of SPM and gain saturation within the device. Furthermore, the SPM and gain saturation will be different depending on the direction of propagation through the device due to the asymmetric waveguide and confinement factor. There is also a dependence of SPM and gain saturation on the properties of the input pulse such as its chirp, duration and energy [22]. In the double-pass configuration, the pulses recoupled into the rear facet of the SOA after a single-pass will have different chirps, durations and energies compared to the original input pulses. In addition, the two-section contact layout means that the current density within the SOA is non-uniform, which again influences the levels of SPM and gain saturation. Lastly, the relatively large and non-uniform current densities applied to the SOA could also induce active region temperature effects that can affect the pulse duration [4].

Figure 6 also indicates that by varying the driving current applied to each section of the SOA, the pulse duration could be tuned within a certain range at a fixed output power. This is a particularly attractive benefit afforded by the two-section contact, since it allows pulse

Optics EXPRESS

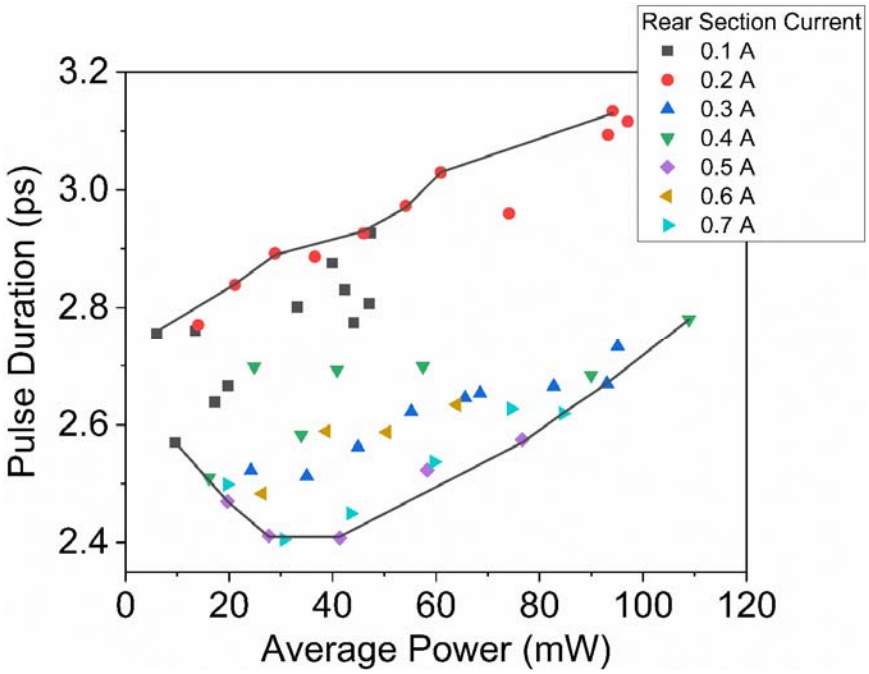

Fig. 6. Plot of pulse duration vs output power of pulse from the double-pass amplifier with the long-pass filter. Black lines indicate upper and lower envelopes of the pulse duration tuning range.

duration to be minimised at a given output power, allowing peak power to be maximised. For example, at a fixed output power of around 60 mW, depending on the driving current applied to the front and rear sections of the SOA, pulses with durations as long as 3 ps and as short as 2.5 ps were observed. This ability to alter the pulse duration at a fixed output power facilitated by the two-section contact could be especially desirable for the double-pass configuration, to help counteract the additional temporal broadening associated with the inherent increased SPM and dispersion.

4. Conclusion and outlook

In summary, we have demonstrated double-pass amplification of picosecond pulses using a tapered SOA. The performance of the double-pass amplifier was compared to a conventional single-pass MOPA setup, revealing a global enhancement both in output power and signal gain from the double-pass amplifier across the entire range of equivalent biasing conditions. A general enhancement of at least 3 dB and a maximum enhancement of 6.8 dB in signal gain was observed in the double-pass amplifier relative to the single-pass, as well as a maximum proportional increase in output power by a factor of 4.1. The highly versatile nature of the double-pass configuration was exploited, and a long-pass filter was introduced in order to inhibit lasing near the ASE peak of the SOA and extend the operating range of the amplifier. This resulted in an increase in the maximum output power of the double-pass amplifier up to 109 mW, a 43% improvement over the maximum power of 76 mW achieved by the single-pass amplifier. Across the new extended range of biasing conditions in common between the single-pass and double-pass amplifier including the long-pass filter, a maximum enhancement in output power of 75 mW was observed along with a general enhancement of 4 dB and a maximum enhancement of 7 dB in the signal gain. Although the combined effects of gain saturation, self-phase modulation

Optics EXPRESS

and chromatic dispersion appeared to be greater in the double pass configuration, the durations of the output pulses were only marginally higher than those observed from the single pass amplifier. Furthermore, the two-section contact layout of the SOA was shown to allow the pulse duration to be minimised at a given fixed output power, allowing peak power to be maximised.

Double-pass amplification affords more flexibility if needed, with additional spatial and spectral shaping possible, for example, with the addition of prism pulse compressors between the SOA and feedback mirror or alternative transmission filters. Additionally, the efficiency and compactness of the double-pass technique could be further explored for better field deployment. A bespoke, low-loss reflective coating could be deposited onto the rear facet of the SOA to minimise coupling losses and tailor feedback for a given application. In this work we also demonstrated the potential advantages of utilising a SOA with a multi-section contact layout, which affords greater flexibility in tuning the characteristics of the output pulses.

The double-pass amplifier configuration that we have presented is a versatile and powerful technique which could become the standard for amplification. The approach presented in this paper could also be applied to further extend the reach of other successful amplification techniques, such as x-CPA (eXtreme Chirped Pulse Amplification) [23], additive pulse amplification [19] and pulse picking [2,24].

Funding

Engineering and Physical Sciences Research Council; Biotechnology and Biological Sciences Research Council; FP7 Information and Communication Technologies (224338); H2020 European Research Council (640537). Supporting data is available at https://researchportal.hw.ac.uk/.

Acknowledgments

The authors would like to thank Innolume GmbH (Germany) for the growth of the QD wafers. The authors would like to thank T. Xu, M. Rossetti and I. Montrosset for stimulating discussions. From III-V Lab the authors would also like to thank M. Tran for SOA processing, Y. Robert for the SOA low-reflectivity coating, E. Vinet and M. Garcia for SOA mounting and M. Ruiz for characterization.

References

1. S. Kono, R. Koda, H. Kawanishi, and H. Narui, "9-kW peak power and 150-fs duration blue-violet optical pulses generated by GaInN master oscillator power amplifier," Opt. Express **25**(13), 14926–14934 (2017).
2. P. Klopp, U. Griebner, M. Zorn, A. Klehr, A. Liero, M. Weyers, and G. Erbert, "Mode-locked InGaAs-AlGaAs disk laser generating sub-200-fs pulses, pulse picking and amplification by a tapered diode amplifier," Opt. Express **17**(13), 10820–10834 (2009).
3. F. C. Cruz, M. C. Stowe, and J. Ye, "Tapered semiconductor amplifiers for optical frequency combs in the near infrared," Opt. Lett. **31**(9), 1337–1339 (2006).
4. T. Ulm, H. Fuchs, J. A. L'huillier, A. Klehr, B. Sumpf, and E. Gehrig, "Amplification of kW peak power femtosecond pulses in single quantum well InGaAs tapered amplifiers," Opt. Commun. **281**(8), 2160–2166 (2008).
5. E. U. Rafailov, M. A. Cataluna, and W. Sibbett, "Mode-locked quantum-dot lasers," Nat. Photonics **1**(7), 395–401 (2007).
6. Y. Ding, R. Aviles-Espinosa, M. A. Cataluna, D. Nikitichev, M. Ruiz, M. Tran, Y. Robert, A. Kapsalis, H. Simos, C. Mesaritakis, T. Xu, P. Bardella, M. Rossetti, I. Krestnikov, D. Livshits, I. Montrosset, D. Syvridis, M. Krakowski, P. Loza-Alvarez, and E. Rafailov, "High peak-power picosecond pulse generation at 1.26 μm using a quantum-dot-based external-cavity mode-locked laser and tapered optical amplifier," Opt. Express **20**(13), 14308–14320 (2012).
7. Y. Ding, A. Alhazime, D. Nikitichev, K. Fedorova, M. Ruiz, M. Tran, Y. Robert, A. Kapsalis, H. Simos, C. Mesaritakis, T. H. Xu, P. Bardella, M. Rossetti, I. Krestnikov, D. Livshits, I. Montrosset, D. Syvridis, M. A. Cataluna, M. Krakowski, and E. Rafailov, "Tunable Master-Oscillator Power-Amplifier Based on Chirped Quantum-Dot Structures," IEEE Photonics Technol. Lett. **24**(20), 1841–1844 (2012).
8. M.-T. Choi, W. Lee, J.-M. Kim, and P. J. Delfyett, "Ultrashort, high-power pulse generation from a master oscillator power amplifier based on external cavity mode locking of a quantum-dot two-section diode laser," Appl. Phys. Lett. **87**(22), 221107 (2005).

Optics EXPRESS

9. C. Weber, L. Drzewietzki, M. Rossetti, T. Xu, P. Bardella, H. Simos, C. Mesaritakis, M. Ruiz, I. Krestnikov, D. Livshits, M. Krakowski, D. Syvridis, I. Montrosset, E. U. Rafailov, W. Elsäßer, and S. Breuer, "Picosecond pulse amplification up to a peak power of 42 W by a quantum-dot tapered optical amplifier and a mode-locked laser emitting at 1.26 µm," Opt. Lett. **40**(3), 395–398 (2015).
10. M. Kuntz, G. Fiol, M. Laemmlin, C. Meuer, and D. Bimberg, "High-Speed Mode-Locked Quantum-Dot Lasers and Optical Amplifiers," Proc. IEEE **95**(9), 1767–1778 (2007).
11. V. Bolpasi and W. v. Klitzing, "Double-pass tapered amplifier diode laser with an output power of 1 W for an injection power of only 200 µW," Rev. Sci. Instrum. **81**(11), 113108 (2010).
12. V. M. Valenzuela, L. Hernández, and E. Gomez, "High power rapidly tunable system for laser cooling," Rev. Sci. Instrum. **83**(1), 015111 (2012).
13. H. Ahmad, M. Z. Zulkifli, N. A. Hassan, A. A. Latif, and S. W. Harun, "High gain S-band semiconductors optical amplifier with double-pass configuration," Laser Phys. **21**(7), 1208–1211 (2011).
14. C. E. Rogers and P. L. Gould, "Nanosecond pulse shaping at 780 nm with fiber-based electro-optical modulators and a double-pass tapered amplifier," Opt. Express **24**(3), 2596–2606 (2016).
15. T. Xu, P. Bardella, M. Rossetti, and I. Montrosset, "Beam propagation method simulation and analysis of quantum dot flared semiconductor optical amplifiers in continuous wave high-saturation regime," IET Optoelectron. **6**(2), 110–116 (2012).
16. S. Riecke, S. Schwertfeger, K. Lauritsen, K. Paschke, R. Erdmann, and G. Tränkle, "23W peak power picosecond pulses from a single-stage all-semiconductor master oscillator power amplifier," Appl. Phys. B: Lasers Opt. **98**(2-3), 295–299 (2010).
17. R. Koda, T. Oki, S. Kono, T. Miyajima, H. Watanabe, M. Kuramoto, M. Ikeda, and H. Yokoyama, "300 W Peak Power Picosecond Optical Pulse Generation by Blue-Violet GaInN Mode-Locked Laser Diode and Semiconductor Optical Amplifier," Appl. Phys. Express **5**(2), 022702 (2012).
18. R. Koda, Y. Takiguchi, S. Kono, H. Watanabe, Y. Hanzawa, H. Nakajima, M. Shiozaki, N. Sugawara, M. Kuramoto, and H. Narui, "Generation of a 2.2 nJ picosecond optical pulse with blue-violet wavelength using a GaInN master oscillator power amplifier," Appl. Phys. Lett. **107**(4), 041116 (2015).
19. M. A. Alloush, R. H. Pilny, C. Brenner, T. Przziwarka, A. Klehr, A. Knigge, G. Tränkle, and M. R. Hofmann, "Mode-locked diode laser with resonant ring amplifier," Proc. SPIE **10682**, 22 (2018).
20. A. F. Forrest, M. Krakowski, P. Bardella, and M. A. Cataluna, "High-power quantum-dot superluminescent tapered diode under CW operation," Opt. Express **27**(8), 10981–10990 (2019).
21. G. P. Agrawal and N. A. Olsson, "Self-phase modulation and spectral broadening of optical pulses in semiconductor laser amplifiers," IEEE J. Quantum Electron. **25**(11), 2297–2306 (1989).
22. M. Y. Hong, Y. H. Chang, A. Dienes, J. P. Heritage, and P. J. Delfyett, "Subpicosecond pulse amplification in semiconductor laser amplifiers: theory and experiment," IEEE J. Quantum Electron. **30**(4), 1122–1131 (1994).
23. K. Kim, S. Lee, and P. J. Delfyett, "1.4 kW high peak power generation from an all semiconductor mode-locked master oscillator power amplifier system based on eXtreme Chirped Pulse Amplification(X-CPA)," Opt. Express **13**(12), 4600–4606 (2005).
24. J. C. Balzer, T. Schlauch, T. Hoffmann, A. Klehr, G. Erbert, and M. R. Hofmann, "Modelocked semiconductor laser system with pulse picking for variable repetition rate," Electron. Lett. **47**(25), 1387–1388 (2011).